Freeze-thaw electrospun PVA-Dacarbazine nanoparticles: preparation, characterization and anticancer evaluation

Luiza Steffens[ab], Bor Shin Chee[a], Dinara Jaqueline Moura[b], Michael Nugent[a*]

a- Athlone Institute of Technology, Materials Research Institute, Athlone, Co. Westmeath, Ireland

b- Laboratory of Genetic Toxicology, Federal University of Health Sciences of Porto Alegre – UFCSPA, Sarmento Leite Street, n° 245, Lab.714, Porto Alegre City, Rio Grande do Sul State, Brazil

* Corresponding author. Address: Athlone Institute of Technology, Dublin road

Athlone, Co. Westmeath, Ireland

E-mail address: MNugent@ait.ie (Michael Nugent)

E-mail addresses: luizasteffens@live.com (L. Steffens), b.schee@research.ait.ie (B.S Chee), dinaram@ufcspa.edu.br (D.J. Moura), MNugent@ait.ie (M. Nugent).

ABSTRACT

Dacarbazine (DTIC) is an antitumor agent that has limited clinical applications due to its insolubility, instability and toxicity to normal cells. One possibility to achieve controlled release is PVA-based NPs. This work presents electrospun NPs that combines PVA and DTIC. The results showed that DTIC NPs had mean particle sizes of 458.2±113.6 nm, suggested the presence of DTIC in an amorphous state and showed a burst *in vitro* drug release followed by a constant release. The cytotoxicity evaluation showed that DTIC NPs were effective against glioblastoma cells. This study indicates that the formulated NPs improved DTIC solubility and efficacy.

Key-words: Electrospinning; Dacarbazine; Nanoparticles; Polyvinyl alcohol; Anticancer activity; Freeze-thaw.

Abbreviations: ANOVA: one-way analysis of variance, ATR-FTIR: attenuated total reflectance Fourier transform infrared spectroscopy, DMEM: dulbeco's modified eagle medium, DMSO: dimethyl sulfoxide, DSC: differential scanning calorimeter, DTIC: dacarbazine, EE%: percentage encapsulation efficiency, FBS: fetal bovine serum, F/T: freeze/thaw, MTIC: methyldiazonium, MTT: 3-(4,5-dimethylthiazol-2-yl)-2,5-diphenyltetrazolium bromide, MW: molecular weight, NP: nanoparticles, OD: optical density, PBS: phosphate-buffered saline, PNPs: polymeric NPs, P-80: polysorbate-80, PVA: polyvinyl-alcohol, Rho-B: rhodamine-B, SEM: scanning electron microscope, Tm: melting point, Tg: glass transition, UV: ultraviolet, XRD: x-ray diffraction.

1. INTRODUCTION

Dacarbazine (DTIC) is an antitumor drug analog of AICA ribonucleotide (5-aminoimidazole-4-carboxamide), which is an intermediate in the formation of inosine monophosphate in the purine biosynthesis [1]. Because of that, DTIC was designed as an antimetabolite originally [1]. Though, given the action of its metabolite, methyldiazonium (MTIC), which methylates DNA, DTIC has a significant cytotoxic activity [1].

Currently, DTIC is used as a chemotherapy drug against metastatic malignant melanoma [2,3]. Furthermore, it is used in combination with different drugs in the treatment of Hodgkin's disease, soft tissue sarcoma and can be used to treat recurrent glioblastoma, neuroblastoma and Kaposi's sarcoma, as an alternative treatment [4,5]. However, DTIC has some serious issues. Firstly, normally the administration route is intravenous, which entails in low patient compliance, given its painful. Moreover, the DTIC absorption in the body is generally inconsistent, slow and partial. Additionally, the drug has poor solubility, instability, photosensitivity and severe toxicity to non-cancerous cells, given that its medical applications are limited [6].

To encapsulate this drug using nanocarriers or nanoparticles (NPs) systems intended for controlled drug delivery is a promising approach to overcome these issues. NPs are nanosized materials that can bypass normal cells while delivering continuous doses of therapeutic substances into tumor cells. Moreover, NPs can improve the chemotherapy solving issues, such as drug resistance, non-specific biodistribution and undesirable side effects [7]. Interesting NPs studies have been managed to the admission of NP-based treatments into clinical trials during the past decade [8].

Due to the capacity to self-assembly and to targeted the tumor, polymeric NPs (PNPs) are one of the most encouraging approaches to use in cancer therapy [9]. PNPs are also biocompatible; they normally present small sizes and the production is simple and with low cost when compared to other drug delivery approaches [9]. PNPs can be separated into biodegradable and non-biodegradable. Biodegradable PNPs

are usually used for drug delivery systems owing to several characteristics, such as low immunogenicity and significant encapsulation. In addition, they can improve some drug characteristics, for example, they can increase the stability, bioavailability and release rate of the drug [9]. Given the low systemic toxicity of the PNPs as drug delivery systems, they are an appropriate option in the delivery of hydrophobic medicines as DTIC. In this context polyvinyl alcohol (PVA) is an interesting choice, since this polymer is very biocompatible, non-toxic and has an outstanding history when used as bioproducts [10,11,12]. Because of appropriate mechanical and swelling features, freeze/thaw (F/T) hydrogels can be produced with significant potential for using as delivery systems. These F/T hydrogels are produced by submitting PVA/water solutions to cycles of freezing and thawing; this process results in the formation of stable gels by the presence of crystalline regions [13,14].

Among the diverse categories of nanotechnologies to produce NPs, electrospinning has proved its effectiveness in producing nanoproducts in a one-step straightforward manner [15]. Even though the electrospinning method has an easy implementation, this method also has a notable potential for generating NPs with multifaceted structures in an industrialized scale [16]. In addition, electrospinning can produce PNPs with different sizes, porosity, drug packing and release rate, leading to an opportunity of adapting the drug release rate for each usage [17].

The present study presents the first production and characterization of F/T electrospun PVA NPs for the encapsulation and controlled release of DTIC that could eventually be used to improve drug stability, efficacy, and safety in cancer treatment.

2. MATERIALS AND METHODS

2.1 Materials

PVA (MW 13000-23000, 90% hydrolyzed), Dacarbazine (DTIC), Rhodamine B (Rho-B), Ethanol, Acetic Acid, Methanol, Dimethyl sulfoxide (DMSO), Polysorbate-80 (P-80) and 3-(4,5-dimethylthiazol-2-yl)-2,5-diphenyltetrazolium bromide (MTT) were purchased from Sigma e Aldrich (Arklow, Ireland). Trypan blue, phosphate buffered saline (PBS), Dulbecco's modified eagle medium (DMEM), fetal bovine serum (FBS), L-glutamine, trypsin-EDTA and penicillin/streptomycin and were purchased from Gibco-BRL

(Dublin, Ireland).

2.2 PVA nanoparticles preparation

PVA solutions were prepared by dissolving PVA (molecular weight of 13,000-23,000) at 10% concentration (wt/vol) in distilled water, at 90°C with continuous stirring until the complete solubilization of PVA was accomplished. Then, for samples containing drugs the temperature was decreased to 50°C and dacarbazine (10 mg) or rhodamine (10 mg) were mixed. After the solutions cooled down, ethanol (10%) and polysorbate-80 (1%) were added. Then, the solutions were frozen (-80°C) for 1 h (Innova U535 freezer, New Brunswick Scientific, Edison, NJ). The samples were then thawed to room temperature. The solutions were electrospun using a blunt-end 20-gauge needle and a flow rate of 0.5 ml/h. 12 kV was applied to the tip of the needle and the needle tip to collector distance was 5 cm. For comparison proposes, two PVA solutions in the same concentration were prepared. One solution, PVA hydrogel, was submitted to the FT process and let dry at room temperature, the other solution, PVA film, was let it dry at room temperature without the FT process.

2.3 Determination of viscosity

The viscosity of the hydrogel solutions was measured by using a Discovery HR-2 rheometer (TA instruments, DE, USA). As the heating component, a Peltier plate was used at a temperature ramp and a 60 mm steel plate was used as the top geometry. The solutions were transferred into the plate of rheometer and viscosity of the samples was analyzed as a function of the temperature ramp (10-40°C).

2.4 Analysis of particle size and morphology

The NPs shape was studied using a scanning electron microscope (Tescan mira XMU SEM, TESCAN, Brno, CZ) in back scattered electron mode. The magnifications used ranged from 10kX to 80kX. The samples were sputtered with gold for 110 s at 0.1 mBar vacuum before testing. After the images recording, ImageJ software was used (ImageJ Version 1.48v) to determine the NP mean diameter. More than 200 DTIC NPs were evaluated.

2.5 Determination of loaded amount and encapsulation efficiency of DTIC

To evaluate the percentage encapsulation efficiency (EE%) of the loaded DTIC in the NPs, DTIC-NPs were completely dissolved in dH_2O to ensure that only free drug was quantified and the solutions were filtered. The amount of released DTIC was measured by ultraviolet (UV) light on Shimadzu UV 1280 spectrometer at 323 nm. The EE% of the DTIC was determined using a calibration curve of DTIC and the equation below:

$$EE(\%) = \frac{actual\ amount\ of\ loaded\ DTIC\ in\ NPs}{theoretical\ amount\ of\ loaded\ DTIC\ in\ NPs} X100$$

In this equation the actual amount of released DTIC in NPs was measured and the theoretical amount was calculated according to the concentration of DTIC added in the PVA solution.

2.6 Fourier transform infrared spectral study

Aiming to investigate the possible chemical interactions between DTIC and PVA after electrospray, attenuated total reflectance Fourier transform infrared spectroscopy (ATR-FTIR) was used. The analysis was accomplished using a Perkin Elmer Spectrum One fitted with a universal ATR sampling accessory (Perkin Elmer, Dublin, Ireland). The data were analyzed in the range of 4000-650 cm^{-1} using 4 scans per sample. Following investigation was performed using Spekwin32software.

2.7 Differential scanning calorimetry

The physical state of DTIC after encapsulation in PVA NPs was examined using differential scanning calorimeter (DSC). The results were acquired by using a DSC TAQ2000 (TA instruments, DE, USA). The samples weights were measured and then, they were fitted in sealed aluminum pans, with weights between 5 and 10 mg. A temperature ramped from 20°C to 270°C was tested at a rate of 10°C per min with an empty pan as a reference. The results were plotted as a function of heat flow (W/g) against temperature (°C).

2.8 X-Ray Diffraction analysis

The molecular structure of the samples was examined by X-ray diffraction (XRD) analysis. The X-ray diffractograms were obtained in an X'Pert MPD PRO diffractometer (PANalytical, Netherlands) with Cu Kα radiation (λ = 1.54060 Å) in the 2θ range of 10–60◦. The intensity and voltage applied were 40 mA and 40 kV, respectively.

2.9 *In vitro* drug release studies

Drug dissolution profiles were achieved using a Distek Model 2500 Dissolution System (Distek, Inc., USA). A phosphate buffer solution (pH 7.4 at 37°C) was used to test the samples. The stir rate was set to 50 rpm with 900 ml of buffer used per sample vessel. Samples were taken at set periods and evaluated by UV light on Shimadzu UV 1280 spectrometer at 323 nm.

2.10 Cell uptake

The glioblastoma cells (U87) were kindly provided by Dr. Brona Murphy (Department of Physiology and Medical Physics, Royal College of Surgeons in Ireland). Cells were cultured in 10% FBS DMEM with antibiotics at 37°C in a humidified atmosphere containing 5% CO_2. The cellular uptake of NPs was studied in a time-dependent way. Frist, Rhodamine-B, a fluorescent probe, was loaded in the NPs. Then, glioblastoma cells were treated with Rho-B-NPs (1mg/mL) and incubated for different time points. After treatment, cells were washed with PBS and completely dissolved in Acetic Acid:Ethanol:dH2O (1:49:50, respectively). The NPs uptake was acquired using a plate reader (BioTek Synergy HT, Swindon, UK) at 543 nm. The quantity of NPs into the cells was calculated using the subsequent formula:

$$\%\ cellular\ uptake = \frac{amount\ of\ Rho - B\ taken\ up\ by\ cells}{total\ amount\ of\ Rho - B\ added}\ X\ 100$$

Furthermore, the cells were seeded in six-well culture plates and then, incubated with Rho-B-NPs or Rho-B for 2, 6 and 24 hours. After treatment, cells were washed with PBS and fixed in methanol. Fluorescence images were acquired using the Leica DM 2000 confocal microscope with an x40 oil lens (Leica Microsystems, Ireland). Image acquisition was performed by LAS V3.8 software (Leica).

2.11 Cell viability evaluation

The NPs cytotoxicity was analyzed by using MTT colorimetric assay. U87 cells (1×10^4 per well) were seeded in 96-well culture plates and incubated at standard conditions. Cells were exposed to different concentrations of blank NPs and DTIC-loaded NPs for 24 hours or 5 days. Cells were then treated with MTT reagent for 3 hours at 37°C. To dissolve the formazan crystals, DMSO was added to each well. The absorbance was recorded at 540 nm in a plate reader (BioTek Synergy HT, Swindon, UK), and

percentage of cell viability was calculated. The cytotoxicity of blank NPs was evaluated using 3T3 cells (as a control cell line).

2.12 Statistical analysis

The results were expressed as mean value ± SD. The statistical analysis was executed using one-way analysis of variance (ANOVA) following by Tukey posttest or two-way ANOVA following by Bonferroni posttest using GraphPad Prism 5 software (La Jolla, CA, USA). P-value (<0.05) were considered to be statistically significant.

3. RESULTS AND DISCUSSION

3.1 Fabrication and characterization of electrospun nanoparticles

To establish a controllable drug delivery system, DTIC-encapsulated NPs were fabricated using the electrospray method. Electrospray removes the emulsion step that can cause sensitive drugs to lose their activity, what differs from other methods to produce NPs [18]. Electrospinning equipment can produce NPs and nanofibers, therefore polymer concentration of the solution imposes the assemblies of the resulting nanoproduct. Spherical particles were observed at lower solution concentrations. When higher concentrations were used the nanofibers with beads started to be visible on the support material (data not shown). To find the optimal solution, it is important to adjust the viscosity of the solution. Felice et al. built a solution screening using two PVAs with different molecular weights (MW) (low and high) and several concentrations. They suggested that the morphology transitions of the nanoproduct occur due to changes of MW or polymer concentration and that the leading underlying mechanism that effects the variation is the number of chains entanglements which accordingly causes modifications in solution viscosity. For electrospraying, it is essential to prepare solutions that have concentrations varying from the critical chain overlap concentration to entanglement concentration. If the concentration is excessively low there are not adequate chain entanglements inside a drop to stabilize the NP development and it loses its structure, however, if the concentration is high there is an augmented quantity of chain entanglements which serves to stabilize the jet, creating polymeric networks and producing fibers [39].

PVA, an FDA-approved non-toxic hydrophilic polymer, was used to produce the NPs. Given that

decreasing PVA MW, the solubility, flexibility and water sensitivity increase, PVA 13-23 kDa was selected. Moreover, low MW PVA solution presents low viscosity and facilitate the production of a spray [18, 39]. The NPs were coated with polysorbate-80 (P-80) to improve the cell absorption, given that there have been numerous reports of NPs coated with P-80 and these NPs presented a significant improvement in the anticancer drugs delivery to the brain [19,20,21]. DTIC was chosen as a model drug to be combined in the PVA NPs since DTIC is an unstable antineoplastic drug however, it has several anticancer applications.

The characteristics of PNPs should be analyzed under their assembly, mechanical properties and functionalization in generating a worthy drug delivery system. By utilizing PVA and electrospinning, it is possible to produce PNPs with customizable composition, size, drug loading and controlled release rate [17]. However, thermosensitive compounds that are not stable in temperatures around 50°C are not indicated to be used with our preparation method. For comparison proposes, two PVA solutions in the same concentration were prepared (PVA hydrogel that was submitted to F/T process and PVA film). It is important to compare control PVA samples with electrospun samples and evaluated its chemical and behavior modifications, because it is the first time that a NP was produced using electrospray from an F/T solution, and our results suggested that the F/T gave the adequate viscosity to produce NP and, even that the F/T process increases crystallinity of polymers, our NPs showed greatly improved solubility.

To investigate the outcome of PVA concentration different PVA solutions were tested (data not shown) and the F/T 10wt% hydrogel was chosen because had the optimal viscosity to use in the electrospray equipment, since solutions with low viscosity do not have sufficient chain entanglements inside a drop in the Taylor cone to stabilize the NP formation and losing its shape when arriving in the collector plate; while high viscosity, there is an enlarged amount of chain entanglements which stabilizing the spray throughout the process given the increased surface tension, generating nanofibers. Moreover, particle size presents an important dependency on solution viscosity where higher viscosities involve more chain entanglements. Thus, using solutions with high viscosity is possible to obtain larger NPs. Previous studies with PVA NP production showed that low MW PVA is more suitable than high MW PVA for the preparation of electrosprayed NP [39]. Additionally, taking into considerations that sustained release

profile is desired over a shorter one, the concentration of 10wt% provided stable NPs with controlled release.

Figure 1A shows the viscosity of a PVA hydrogel that was submitted to F/T method in comparison with a control PVA hydrogel, the higher viscosity of F/T hydrogel permitted a stable jet flow during the electrospray process (figure 1B). It is well known that PVA hydrogels prepared by F/T methods show improved mechanical strength when compared with most hydrogels given the presence of crystalline regions [13]. These regions function as physical crosslinks [13,14]. Moreover, water solutions are not very suitable for electrospraying due to the high surface tension of the solvent, thus ethanol was added, mainly because of its safety and comparatively low price.

Morphology and particle size play a substantial role in the evaluation of NPs designs [22]. Particle size has an important influence on the release of the drug, given that, smaller the size of the NP, larger the surface area, and consequently faster is the drug delivery [23]. The morphology of the NPs was observed by using SEM (figure 2A and B). The SEM images revealed that the particles were spherical and the average size was 458.2±113.6 nm (figure 2C).

FTIR was used to examine the characteristic chemical band of PVA electrospun NPs. FTIR fingerprints of PVA and DTIC have been reported in the literature [24,25,26]. It is possible to observe in all samples the characteristic bands of PVA. These peaks normally correspond to alcohol and carboxylic acid groups (figure 3). The large peak between 3500 and 3200 cm^{-1} was owing to the stretching O-H. The electrospun process resulted in more defined peaks and increase the 3302 cm^{-1} band which indicates the presence of more hydrogen bonding as compared to hydrogel sample, also 2948, 2850 cm^{-1} peaks are sharper. No significant shift alterations in the major peaks corresponding to PVA can be observed for DTIC NPs when compared to Blank NPs, indicating that there are no chemical interactions between DTIC and PVA. If a band shift is detected this phenomenon is interpreted as the manifestation of changes in the FTIR associated with a specific chemical bond under the influence of molecular interactions [27, 42]. However, the final concentration of DTIC was extremely low (less than 2%) and this could influence in the spectra of the samples given that equipment will detect the major compound easily but no other substances.

The thermal behavior of NPs loaded with DTIC in comparison with thermogram of DTIC powder is demonstrated in figure 4. It is crucial to evaluate the amorphous and crystallinity properties of the samples, since the aim of the NP is to increase the solubility of the drug, therefore the comparison between different approaches (NP, hydrogel, film) with different complexity is important to understand which sample presents the best delivery properties. Additionally, it is interesting to study how the thermal transition of PVA varies after electrospinning process to evaluate if the sample preparation changed the thermal transitions of the polymer. Furthermore, one key aspect is the determination of whether the resulting blend samples results miscible or not is the evaluation of thermal behavior of the NP with DTIC [43].

A thermogram of pure PVA film, PVA hydrogel and PVA NPs is shown in figure 4A. The sharp peak at 220°C represents the melting point (Tm) of the PVA. The α-relaxation which characterizes the glass transition (Tg) of PVA is exemplified by the step change at around 40°C to PVA film and PVA NPs and 59°C to PVA hydrogel. These values are substantially different than the value described in previous studies [28], nevertheless, according to Hirankumar [29] this is due to the incidence of water and its plasticizing consequence on the polymer and for PVA crosslinked hydrogels it was found a Tg in the region of 55°C to 70°C [30]. The β-relaxation that characterizes secondary crystalline relaxation can be observed at 89, 113, 118°C to PVA NPs, PVA hydrogel and PVA film, respectively. These different transitions are probably due to microcrystallites or the evaporation of water [13].

The NPs (figure 4B) also presented an exothermic peak around 180°C probably due to the elimination of adsorbed ethanol and/or water. Another hypothesis is due to the decomposition of residual of organic matter and the hydroxide groups given the chemical rearrangement after the electrospinning process [31] since they lost 15.8%±3.9% (DTIC NPs) and 14.8%±5.1% (Blank NPs) of weight after the DSC process, while the PVA film and the PVA hydrogel lost 4.5%±2.1% and 5.3%±3.4%, respectively. The thermogram of DTIC powder (figure 4C) reveals a sharp exothermic peak at 213°C equivalent to its melting point. This indicates its crystalline state [6]. DTIC NPs shows an endothermic melting peak at 216°C, similar to the blank NPs. This result indicates that, probably, DTIC is adsorbed in semi-crystalline state in the PVA NP construction. It is well known that to modify the physical state of a drug can change

its energy state. In this case, an amorphous state of DTIC can lead to a high energy state and consequently in a high disorder and this can result in an enhanced solubility of DTIC [27,32]. This result is in agreement with the drug release analysis (figure 6).

It is possible to alter, in most polymers, the mechanical characteristics. For instance, given the constant arrangement of the polymer chains, a crystalline polymer probably will degrade and solubilize slower than an amorphous polymer. Nevertheless, amorphous polymers retain reduced mechanical robustness and in another hand, crystalline polymers are usually less suited for use in delivery systems [27]. Given that, the combination of both crystalline and amorphous polymer forms are more suitable to use as drug delivery systems [27].

It is recognized that the PVA polymer shows a semi-crystalline configuration with peaks at the 2 Â angles of 20 and 40◦ [33]. Figure 5 shows a large crystal peak at 2 Â of 20◦ in the PVA film. Given the physical crosslinked F/T process in the PVA hydrogel, where the crystalline domains of PVA act as knots of the gel network increasing the crystallinity [33] the peaks intensity augmented. It is possible to notice a greatly reduced of PVA crystal peaks intensity in the NPs diffractograms. This implies that submitted the hydrogel solution to electrospinning method significantly increased the polymer amorphous region domain. This assumption is in agreement with the DSC results (figure 4). Additionally, it is possible to observe an effective DTIC encapsulation given the absence of crystallinity characteristic peaks of DTIC [6]. During the electrospinning process, there is fast solvent evaporation consequently, the PVA NP sample solidified very quickly, leading to a decrease in the flexibility of DTIC molecules; this is in agreement with prior studies where the authors suggested that some drugs could lose or change the crystalline structure after the electrospun process. Depending on the drug content, these drugs can exist in the amorphous from a combination of amorphous and amorphous solid dispersion [32,34,35,36].

3.2 Drug release and encapsulation efficiency

The resulting drug release from the polymer environment strongly depends on the polymer selected for the matrix composition. In this study, PVA NPs presented a continuous release profile for DTIC during an interval of time. The hydrophobic domain of PVA mainly interacts with the hydrophobic domains of

DTIC, and consequently presents a constant release, while the PVA hydrophilic domains enhanced the diffusion, permeability and degradation on the NPs. DTIC EE(%) was recorded as 59.7%±2.2%, which inferred that greater amount of DTIC was encapsulated into PVA NPs. The sustainability of DTIC in the NPs was studied by using *in vitro* drug release method in physiological pH (7.4) at different intervals (figure 6).

Drug dissolution procedure comprises the transference of individual drug molecules from the solid state into an aqueous environment. The essential factors related to this transference comprise the chemical reactivity, solubility of the drug, system diffusion and hydrodynamic behavior spray [40]. The principle behind Distek drug dissolution is to evaluate the rate of release of a substance from the dosage form. Due to usually NPs are used to enhance the bioavailability of these substances improving the dissolution rate of drugs, the DTIC by itself was also evaluated for comparison proposes. In this experiment sink conditions were used aiming to allow the complete dissolution of DTIC since sufficient media was used to ensure un-impaired dissolution, therefore, after each period of sample collection, the same amount of media was added in the vessel. The release measurements of DTIC, DTIC NPs, DTIC/hydrogel and DTIC/film were recorded as 44.7%, 76.0%, 55.0% and 52.3% at 1 h, respectively. The release profile of the DTIC NPs exhibited an initial burst release (> 50% after 20 min) followed by a constant DTIC release during the following interval. This characteristic could be explained due to the dispersion of DTIC present or adsorbed at the NPs surfaces and also due to the resulted nanopores in the NP shell consequence of the electrospray process during the solvent evaporation [18,34,35].

To achieve an appropriate antitumor treatment, it is necessary to have an initial burst in the drug release following by a continuous release aiming to treat the resistant glioblastoma cells that persist in the primary contact with the drug [36]. Given that, DTIC NPs is appropriate for cancer management and can be used to achieve a continuous release for antitumor treatment. Hence, in spite of the capacity of the DTIC NPs to offer a hydrophilic dissolving environment that improves DTIC dissolution frequency, the distributed state and the solubility of incorporated DTIC, expressively influence the drug release rate [34]. Regarding a poorly water-soluble drug, such as DTIC, the release may be a function of DTIC diffusion and erosion of the PVA in the NP matrix [34].

Aiming to analyze the *in vitro* drug release kinetics, the release profiles of the samples were analyzed using various kinetic models. Given the hypothesis that DTIC was homogeneously dispersed in the NPs, hydrogels and films, the samples were modeled as systems where the drug is assumed to be loaded into PNP by a packing of the drug and polymer [34]. The drug release data were fitted into Higuchi's and Korsmeyer-Peppas models [37] to evaluate which mechanisms were related in DTIC releasing from the samples. As shown in table 1, the curves made by using both kinetic models are in accordance with the release of DTIC from PVA samples ($R^2 > 0.9027$). The exponential factor "n" values were recognized to be between 0.4617 and 0.6324, demonstrating an anomalous drug transport, also known as non-Fickian diffusion-controlled drug release. In this kinetic model, both diffusion and erosion mechanisms are influencing the release [37], while DTIC, the drug by itself, presented an "n" value lower (0.2370), it shows that Fickian diffusion is the main mechanism of DTIC release.

These mathematical models of drug delivery systems have a substantial potential to assist understanding complex bioproducts evaluation, nevertheless, it is improbable to use a unique mathematical model to all types of drug delivery systems [38]. Although the release mechanisms of the PVA matrices need to be more clarified, this study demonstrated that DTIC is released from the electrospun PVA NPs in an initial burst followed by continuous release.

Table 1: Release behavior of DTIC loaded formulations and DTIC in powder form.

Sample		Model		
		Korsmeyer-Peppas		Higuchi
DTIC	n	0.2370	K	33.6480
	R^2	0.7357	R^2	0.8722
DTIC NP	n	0.5543	K	10.3000
	R^2	0.9628	R^2	0.9766
DTIC	n	0.6324	K	48.8800
Hydrogel	R^2	0.9840	R^2	0.9299
DTIC PVA	n	0.4617	K	17.6220

R^2	0.9043	R^2	0.9027

Where, R^2 = regression coefficient, n = release exponent, K = Higuchi rate constant.

3.3 Cell uptake profile

To explore the cellular uptake potential of the NPs, DTIC was replaced with Rho-B. Rho-B is commonly used to analyze the NP behavior in cell culture, given that fluorescence probes enable researches to evaluate cell uptake of substances and particles [44,45]. However, its evaluation provides only an estimation of the behavior of drug delivery systems. As seen from figure 7A, Rho-NPs showed significant uptake mostly after 1 hour of treatment and a continuous uptake until 24 h after.

By using fluorescent microscopy, the cellular uptake was additional confirmed. Nuclei were stained with SYBR Green and a rhodamine-B solution was used as control (figure 7B and C). It is possible to observe that the cells exhibited a shiny fluorescence after 2 hours of treatment and, although it is not statistically significant, given the controlled release of the PVA NPs, after 6 and 24 hours, the fluorescence intensity was higher in the Rho-NP treated cell when compared with the cell treated with a Rho solution.

3.4 Cytotoxicity assay

Aiming to evaluate if the Blank NP could induce toxicity to normal cells (non-tumoral), 3T3 murine cell line was used to ensure that PVA NP is harmless and it could be used without cause side effects. The cells were treated with NPs at four different concentrations and incubated during 24 hours or 5 days. Figure 8A shows that blank NPs did not induce substantial toxicity when compared to the negative control (NC), given that the cell viability endured around 80% in all concentrations. This result indicates that the blank NPs are biocompatible and are appropriate for systemic administration in the cancer therapy.

The cytotoxic effect of DTIC NPs was estimated in U87 glioblastoma cancer cells by using MTT assay (figure 8B and C). The cytotoxic effect of DTIC NPs was estimated in U87 glioblastoma cancer cells by using MTT assay (figure 8B and C). The results showed a concentration (dose) dependent *in vitro* where the cytotoxic effect was obtained by the specific increase in the amount of tested substances. It was observed that after 24 hours, DTIC treatments were statistical more effective than DTIC NP in the concentrations of 0.2 and 0.6 mg/mL, however after 5 days of treatment DTIC NP treatments were more

cytotoxic being statically significant in the concentration of 0.8 mg/mL. The concentration of 0.8 mg/mL was selected to test the Blank NPs. Moreover, after the 5-day treatment, the IC50 value of DTIC NP was 0.23 mg/mL and the IC50 of DTIC was 0.32 mg/mL, indicating that the NPs improved the efficacy of DTIC after prolonged exposure. It was possible to observe that after 5 days of treatment cells were detaching from the bottom of the plate (figure 8C). Moreover, the DTIC treatment of 0.2 mg/mL image suggest a formation of cell agglomerates, this is a typical protection mechanism of cancer cells related to stem-like properties. The same is not possible to perceive with the NP treatment, this may indicate that the NPs treatment can modify cell morphology. However, more experiments are needed to prove this hypothesis. These results indicate that cells are able to repair the damage induced by DTIC after its treatment, however, probably given the slower release of the NPs, cells are continuing to be treated for a prolonged period and are not able to perform a proper repair.

Despite the extensive research to design efficient drug delivery treatments, drug efficacy in treating tumor cells, especially glioblastomas, remains restricted by the relatively trivial quantity of drug distribution and release in existing systems. Given that, these results suggest that the DTIC NPs have a considerably anticancer potential against glioblastoma cells.

Our future work aims to evaluate these promising NPs *in vivo* via intranasal route for direct nose-to-brain delivery of drugs since the brain blood barrier (BBB) presents a severe limitation to administer pharmacological agents to the brain. This barrier restricts the access of 98% of small substances and practically 100% of large substances to the brain [41]. Drugs administrated to the nasal cavity can be directly transported to the brain, bypassing the BBB altogether. This route is very promising in the delivery of drugs given that it can significantly decrease the systemic toxicity and it can make possible NP to reach the tumor site in therapeutic concentrations [41].

4. CONCLUSION

DTIC was effectively entrapped in PVA NPs by using electrospinning method. The NPs particle size distribution indicated an average size of 458.2±113.6 nm, and the NPs were spherical. It could be established from characterization analysis that DTIC NPs were in an amorphous state. The cytotoxicity

evaluation showed that DTIC NPs were more effective against glioblastoma cells than DTIC solution. It can be concluded that F/T electrospun PVA NPs show the potential drug release system of hydrophobic DTIC by improving its solubility and its cytotoxicity in glioblastoma cells. The future studies will incorporate *in vivo* evaluation and further refinement of the process.

Acknowledgments

This study was supported in parts by grants from the Athlone Institute of Technology research and development funding, GOI-IES (Government of Ireland International Education Scholarship) and CAPES (Coordenação de Aperfeiçoamento de Pessoal de Nível Superior, Brazil). We thank Mr. Zhi Cao (Material Research Institute, Athlone Institute of Technology) and Dr. Wynette Redington (Bernal Institute, University of Limerick) for assistance with SEM and XRD analysis, respectively.

Conflict of Interest

The authors declare that there are no conflict of interest.

Statement of authors' contributions to manuscript

L.S and B.S.C conducted the experiments; L.S., D.J.M. and M.N. wrote the paper. All authors read and approved the final manuscript.

References

[1] Shealy, F. Y. Syntheses and biological activity of 5-aminoimidazoles and 5-triazenoimidazoles. *J. Pharm. Sci.* **1970**, 59(11), 1533-1538.

[2] Spieth, K.; Kaufmann, R.; Dummer, R.; Garbe, C.; Becker, J. C.; Hauschild, A.; Tilgen, W.; Ugurel, S.; Beyeler, M.; Bröcker, E. B.; et al. Temozolomide plus pegylated interferon alfa- 2b as

first-line treatment for stage IV melanoma: a multicenter phase II trial of the Dermatologic Cooperative Oncology Group (DeCOG). *Ann Oncol*. **2008**, 19(4), 801–806.

[3] Schadendorf, D.; Ugurel, S.; Schuler-Thurner, B.; Nestle, F. O.; Enk, A.; Bröcker, E. B.; Grabbe, S.; Rittgen, W.; Edler, L.; Sucker, A.; et al. Dacarbazine (DTIC) versus vaccination with autologous peptide-pulsed dendritic cells (DC) in first-line treatment of patients with metastatic melanoma: a randomized phase III trial of the DC study group of the DeCOG. *Ann Oncol*. **2006**, 17(4), 563–570.

[4] Al-Badr, A. A. & Alodhaib, M. M. Chapter Four – Dacarbazine. *Profiles Drug Subst. Excip. Relat. Methodol*. **2016**, 41, 323-377.

[5] Fazeny-Dörner, B.; Veitl, M.; Wenzel, C.; Rössler, K.; Ungersböck, K.; Dieckmann, K.; Piribauer, M.; Hainfellner, J.; Marosi1, C. Survival with dacarbazine and fotemustine in newly diagnosed glioblastoma multiforme. *British J. of Cancer*. **2003**, 88, 496-501.

[6] Di Bei, J.M. & Bi-Botti, C. Y. Formulation of Dacarbazine-Loaded Cubosomes—Part I: Influence of Formulation Variables. *AAPS PharmSciTech*. **2009**, 10(3), 1032-1039.

[7] Bahrami, B.; Hojjat-Farsangi, M.; Mohammadi, H.; Anvari, E.; Ghalamfarsa, G.; Yousefi, M.; Jadidi-Niaragh, F. Nanoparticles and targeted drug delivery in cancer therapy. *Immun Letters*. **2017**, 190, 64-83.

[8] Bombelli, F. B.; Webster, C. A.; Moncrieff, M.; Sherwood, V. The scope of nanoparticle therapies for future metastatic melanoma treatment. *Lancet Oncol.* **2014**, 15(1), 22-32.

[9] Pourgholi, F.; Hajivalili, M.; Farhad, J. N.; Kafil, H. S.; Yousefi, M. Nanoparticles: Novel vehicles in treatment of Glioblastoma. *Biomedic&Pharmacot*. **2016**, 77, 98-107.

[10] Chen, W.; Achazi, K.; Schade, B.; Haag, R. Charge-conversional and reduction-sensitive poly(vinyl alcohol) nanogels for enhanced cell uptake and efficient intracellular doxorubicin release. *J. Controlled Release*. **2015**, 205, 15-24.

[11] De Lima, G. G.; Campos, L.; Junqueira, A.;. Devine, D. M.; Nugent, M. J. D. A novel pH-sensitive ceramic-hydrogel for biomedical applications. *Polym Advan Tech*. **2015**, 26, 1439-46.

[12] Canillas, M.; De Lima, G. G.; Rodrıguez, M. A.; Nugent, M. J. D. Bioactive Composites Fabricated by Freezing-Thawing Method for Bone Regeneration Applications. *Polym Phys*. **2016**, 54, 761-73.

[13] Nugent, M. J. D.; Hanley, A.; Tomkins, P. T.; Higginbotham, C. Investigations of a novel freeze-thaw process for the production of drug delivery hydrogels. *J. of Mat. Sci.: Mat. In Med.* **2005**, 16, 1149-1158.

[14] Mc Gann M. J.; Higginbotham, C. L.; Geever, L.M.; Nugent, M. J. The systhesis of novel pH-sensitive poly(vinyl alcohol) composite hydrogels using a freeze/thaw process for biomedical applications. *Inter. J. of Pharm*. **2009**, 372, 154-161.

[15] Liu, Y.; Hou, C.; Jiao, T.; Song, J.; Zhang, X.; Xing, R.; Zhou, J.; Zhang, L.; Peng, Q. Self-assembled AgNP-containing nanocomposites constructued by electrospinning as efficient dye photocatalyst materials for wastewater treatment. *Nanomaterials*. **2018**, 8, 35.

[16] Liu, X.; Shao, W.; Luo, M.; Bian, J.; Yu, D-G. Electrospun Blank Nanocoating for Improved Sustained Release Profiles from Medicated Gliadin Nanofibers. *Nanomaterials*. **2018**, 8(4):184.

[17] Zhang, J.; Wang, X.; Liu, T.; Liu, S.; Jing, X. Antitumor activity of electrospun polylactide nanofibers loaded with 5-fluorouracil and oxaliplatin against colorectal cancer. *Drug Delivery*. **2016**, 23(3), 784-790.

[18] Cao, Y.; Liu, F.; Chen, Y.; Yu, T.; Lou, D.; Guo, Y.; Li, P.; Wang, Z.; Ran, H. Drug release from core-shell PVA/silk fibroin nanoparticles fabricated by one-step electrospraying. *Sci. Rep*. **2017**, 7, 11913.

[19] Bagad, M. & Khan, Z. A. Poly(n-butylcyanoacrylate) nanoparticles for oral delivery of quercetin: preparation, characterization, and pharmacokinetics and biodistribution studies in Wistar rats. *Inter. J. of Nanomedicine*. **2015**, 10, 3921-3935.

[20] Wilson, B.; Samanta, M. K.; Santhi, K.; Kumar, K. P.; Paramakrishnan, N.; Suresh, B. Poly(n-butylcyanoacrylate) nanoparticles coated with polysorbate 80 for the targeted delivery of Rivastigmine into the brain to treat Alzheimer's disease. *Brain Res.* **2008**, 1200, 159-168.

[21] Gulyaev, A. E.; Gelperina, S. E.; Skidan, I. N.; Antropov, A. S.; Kivman, G. Y.; Kreuter, J. Significant transport of doxorubicin into the brain with polysorbate 80-coated nanoparticles. *Pharm Res*. **1999**, 16(10), 1564-1569.

[22] Zeng, Z.; Yu, D.; He, Z.; Liu, J.; Xiao, F. X.; Zhang, Y.; Wang, R.; Bhattacharyya, D.; Tan, T. T. Graphene Oxide Quantum Dots Covalently Functionalized PVDF Membrane with Significantly-Enhanced Bactericidal and Antibiofouling Performances. *Sci. Rep*. **2016**, 6, 20142.

[23] Hafeez, A. & Kazmi, I. Dacarbazine nanoparticle topical delivery system for the treatment of melanoma. *Sci. Rep*. **2017**, 7, 16517.

[24] Mansur, H.S.; Sadahira, C.M.; Souza, A.N.; Mansur, A.A.P. FTIR spectroscopy characterization of poly(vinyl alcohol) hydrogel with different hydrolysis degree and chemically crosslinked with formaldehyde. *Mater. Sci. Eng. C*. **2008**, 28, 539-548.

[25] Hassan, C. M. & Peppas, N. A. Structure and Applications of Poly(Vinyl Alcohol) Hydrogels Produced by Conventional Crosslinking or by Freezing/Thawing Methods. *Adv. in Pol. Sci*. **2000**, 153, 37-65.

[26] Gunasekaran, S.; Kumaresan, S.; Arunbalaji, R.; Anand, G.; Srinivasan, S. Density functional theory study of vibrational spectra, and assignment of fundamental modes of dacarbazine. *J. Chem. Sci*. **2008**, 120, 315-324.

[27] El-Feky, G. S.; El-Rafie M. H.; El-Sheikh, M. A.; El-Naggar, M. E.; Hebeish, A. Utilization of crosslinked starch nanoparticles as a carrier for indomethacin and acyclovir drugs. *J. Nanomed. Nanotechnol*. **2015**, 6, 254.

[28] Maurer, J.; Eustace, D.; Ratcliffe, C. Thermal characterization of poly(acrylic acid). *Macrom*. **1987**, 20, 196-202.

[29] Hirankumar, G.; Selvasekarapandian, S.; Kuwata, N.; Kawamura, J.; Hattori, T. Thermal, electrical and optical studies on the poly(vinyl alcohol) based polymer electrolytes. *J. Power Sources*. **2005**, 144, 262-267.

[30] Hatakeyema, T.; Uno, J.; Yamada, C.; Kishi, A.; Hatakeyama, H. Gel–sol transition of poly(vinyl alcohol) hydrogels formed by freezing and thawing. *Thermochimica Acta*. **2005**, 431(1-2):144-148.

[31] Dejene, F. B.; Ali, A. G.; Swart, H. C. Reinhardt, B.; Roro, K.; Coetsee, L.; Duvenhage, M-M. Optical properties of ZnO nanoparticles synthesized by varying the sodium hydroxide to zinc acetate molar ratios using a sol-Gel process. *Cent. Eur. J. Phys*. **2011**, 9(5), 1321-1326.

[32] Lopez, F. L.; Shearman, G. C.; Gaisford, S.; Williams, G. R. Amorphous Formulations of Indomethacin and Griseofulvin Prepared by Electrospinning. *Mol. Pharmaceutics*. **2004**, 11(12), 4327-4338.

[33] Ricciardi, R.; Auriemma, F.; De Rosa, C.; Lauprêtre, F. X-ray diffraction analysis of poly(vinyl alcohol) hydrogels, obtained by freezing and thawing techniques. *Macromolecules*. **2004,** 37(5), 1921-1927.

[34] Li, X.; Kanjwal, M. A.; Lin, L.; Chronakis, I. S. Electrospun polyvinyl-alcohol nanofibers as oral fast-dissolving delivery system of caffeine and riboflavin. *Col. and Surf. B: Biointer*. **2013**, 103, 182-188.

[35] Chen, P.; Wu, Q-S.; Ding, Y-P.; Chu, M.; Huang, Z-M.; Hu, W. A controlled release system of titanocene dichloride by electrospun fiber and its antitumor activity in vitro. *Eur. J. Pharm. Biopharm*. **2010**, 76, 413-420.

[36] Vashisth, P.; Singh, R. P.; Pruthi, V. A controlled release system for quercetin from biodegradable poly(lactide-co-glycolide)-polycaprolactone nanofibers and is in vitro antitumor activity. *Bio. and Comp. Pol*. **2015**, 1-13.

[37] Budiasih, S.; Jiyauddin, K.; Logavinod, N.; Kaleemullah, M.; Jawad, A.; Samer, A. D.; Fadli, A.; Eddy, Y. Optimization of polymer concentration for designing of oral matrix controlled release dosage form. *UK J. of Pharm. and Biosci*. **2014**, 5, 54-61.

[38] Siepmann, J. & Siepmann, F. Mathematical modeling of drug delivery. *Inter. J. of Pharm*. **2008**, 364, 328-342.

[39] Felice, B.; Prabhakaran, M. P.; Zamani, M.; Rodríguez, A. P.; Ramakrishna, S. Electrosprayed poly(vinyl alcohol) particles: preparation and evaluation of their drug release profile. *Polym. Int*. **2015**, 64: 1722-1732.

[40] Blanchard, J.; Sawchuk, R. J.; Brodie, B. B. (eds): Principles and Perspectives in Drug Bioavailability. Basel, Karger, **1979**, pp 20-58.

[41] Crowe, T. P.; Greenlee, H. W.; Kanthasamy, A. G.; Hsu, W. H. Mechanism of intranasal drug delivery directly to the brain. *Life Sci*. **2018**, 195: 44-52.

[42] Ryu, S. R.; Noda, I.; Jung, Y. M. What is the origin of positional fluctuation of spectral features: true frequency shift or relative intensity changed of two overlapped bands? *Appl. Spectrosc*. **2010**, 64: 1017-1021.

[43] Guirguis, O. W.; Moselhey, M. T. H. Thermal and structural studies of poly(vinyl alcohol) and hydroxypropyl celulose blends. *Natural Sci*. **2012**, 4: 57-67.

[44] Kiziltepe, T.; Ashley, J. D.; Stefanick, J. F.; Qi, Y. M.; Alves, N. J.; Handlogten, M. W.; Suckow, M. A.; Navari, R. M.; Bilgicer, B. Rationally engineered nanoparticles target multiple myeloma cells, overcome cell-adhesion-mediated drug resistance, and show enhanced efficacy in vivo. *Blood Cancer J*. **2012**, 2, e65.

[45] Liu, K.; Wang, Z.; Wang, S.; Liu, P.; Qin, Y.; Ma, Y.; Li, X..; Huo, Z. Hyaluronic acid-tagged sílica nanoparticles in colon câncer therapy: therapeutic efficacy evaluation. *Int. J. of Nanomedicine*. **2015**, 10: 6445-6454.

List of Figures:

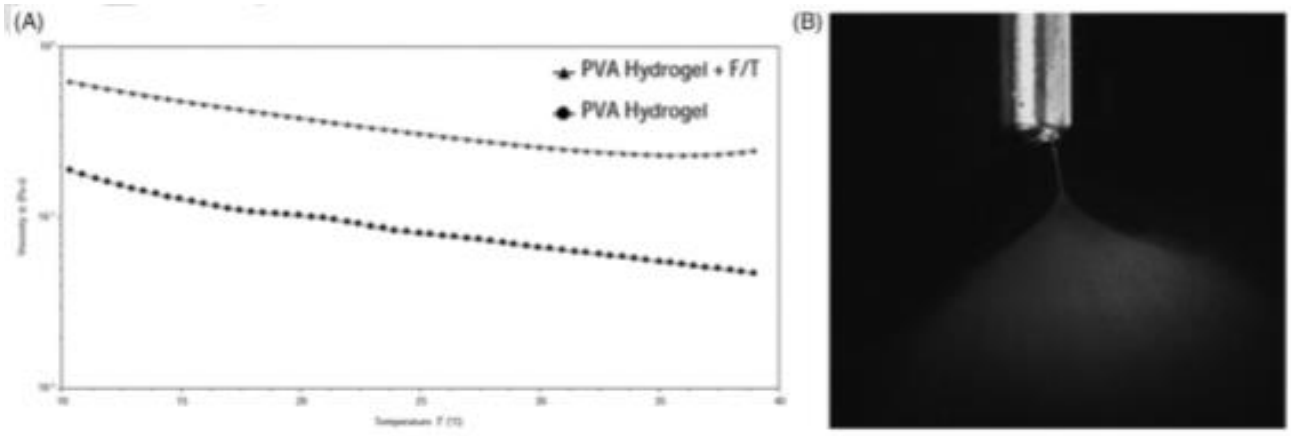

Figure 1: Viscosity analysis of the hydrogel solutions **(A)** Rheometer analysis of hydrogels viscosity **(B)** Taylor cone and resulting spray emanating from the needle tip at 12 kV (image taken with FlyCapture2 2.8.3.1 Software by Point Grey Research, Inc.).

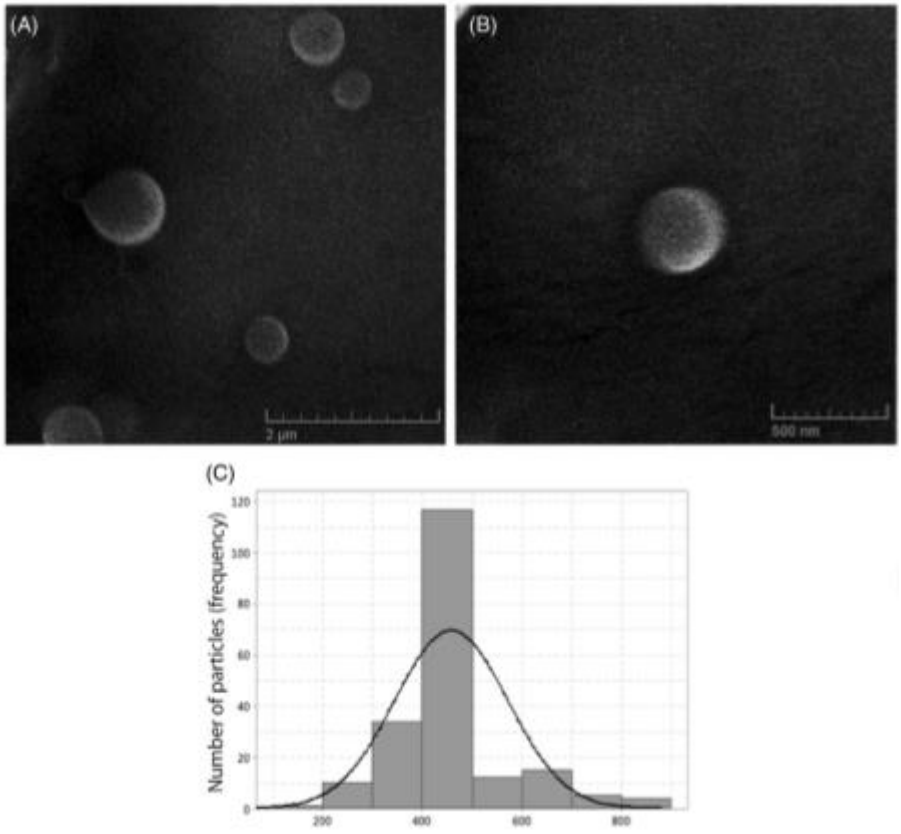

Figure 2: Characterization of the NPs **(A)** SEM images of NPs with 30kx of magnification **(B)** SEM images of NPs with 80kx of magnification **(C)** Particle size distribution of NPs.

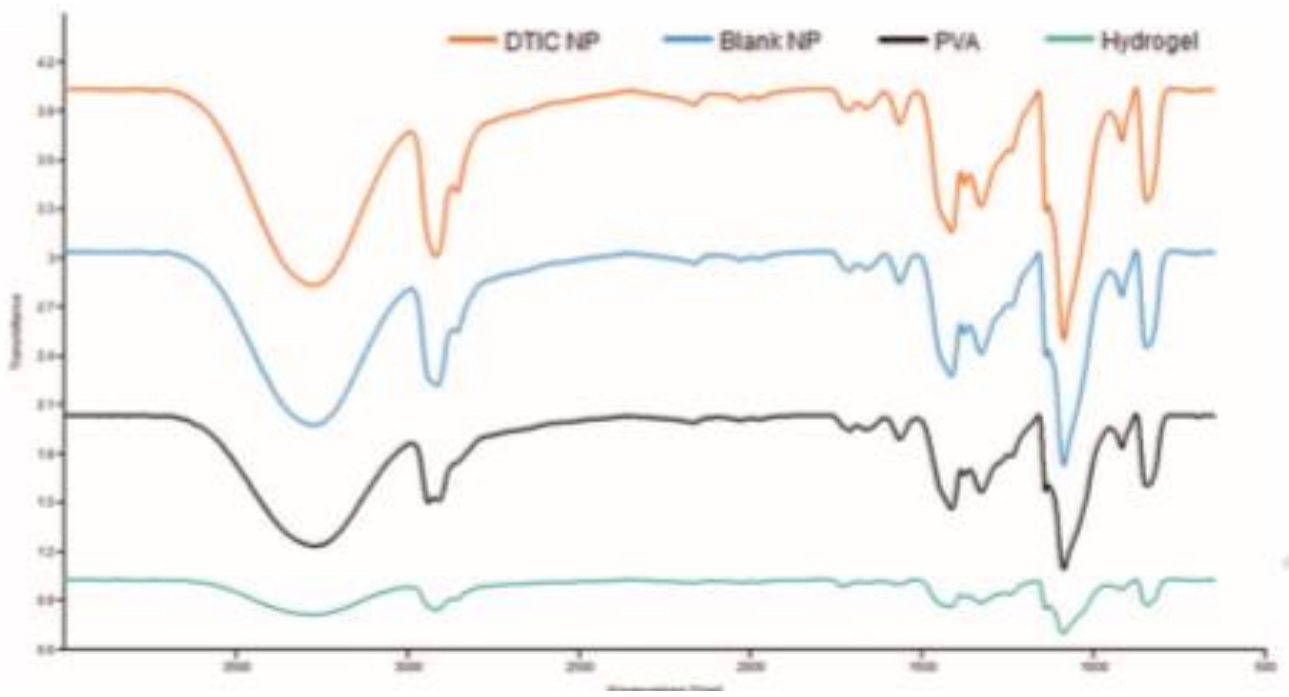

Figure 3: FTIR spectra of the PVA film (black line), PVA Hydrogel (green line), Blank NPs (blue line), DTIC NPs (orange line).

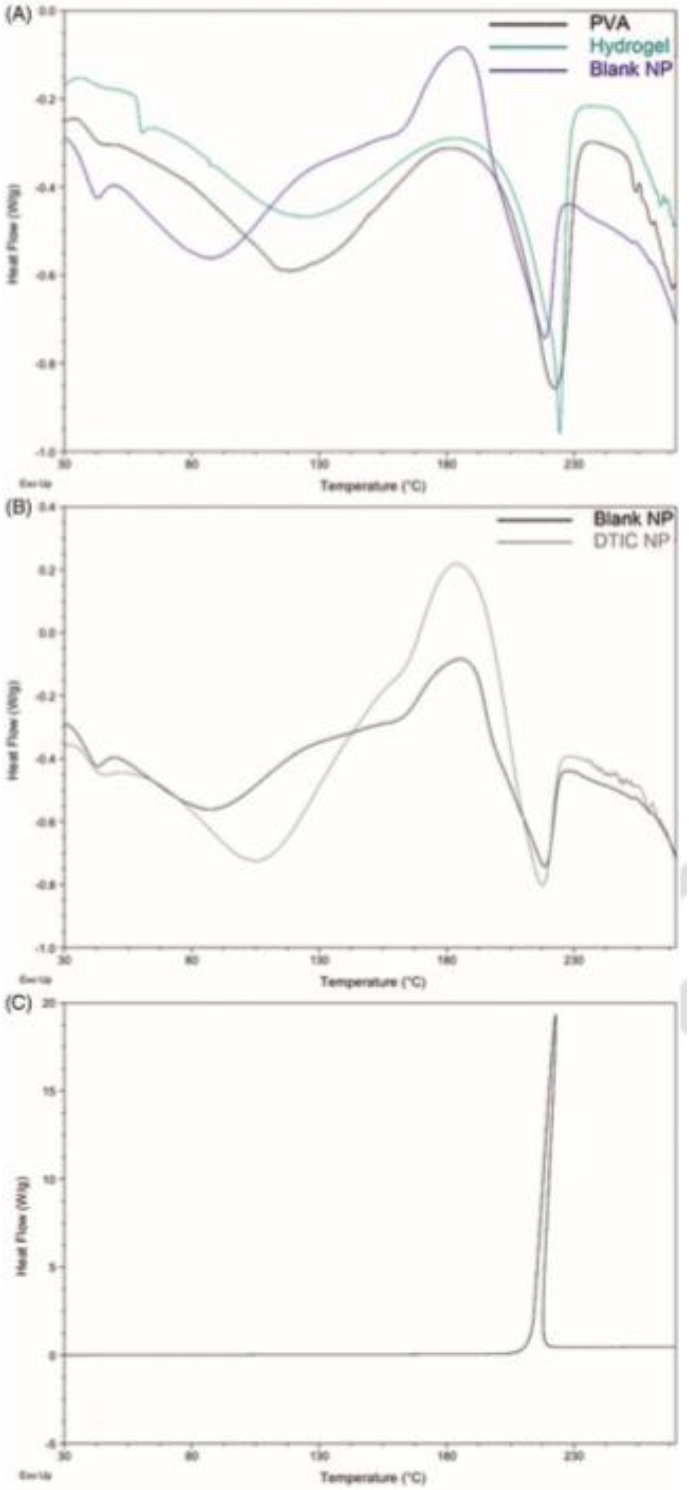

Figure 4: DCS curve obtained from **(A)** PVA film (black line), PVA Hydrogel (green line) and Blank NP (blue line) **(B)** Blank NPs (black line) and DTIC NPs (gray line) **(C)** DTIC in powder form.

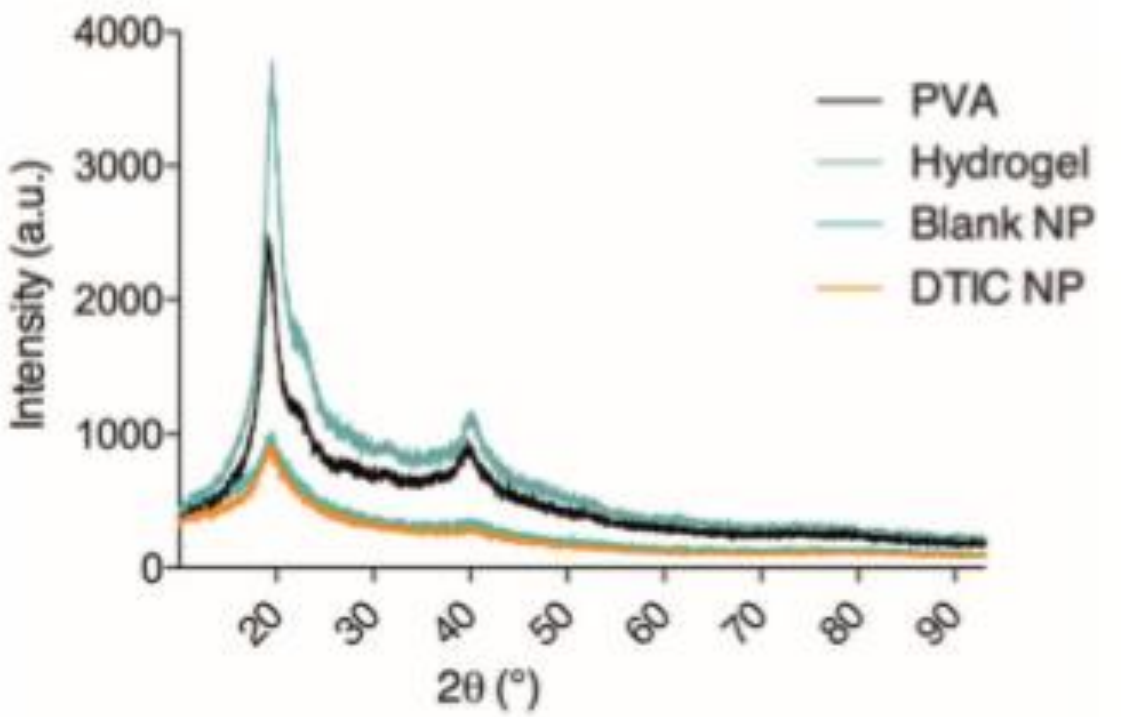

Figure 5: X-Ray diffraction of PVA film, PVA hydrogel, Blank NPs and DTIC loaded NPs.

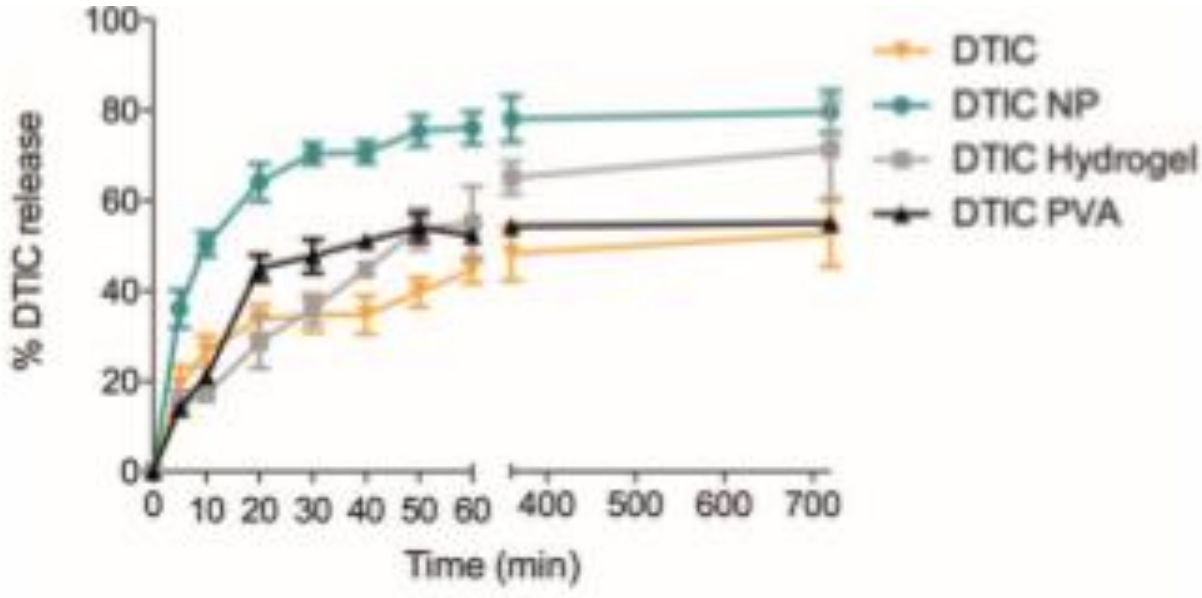

Figure 6: DTIC loaded formulations and DTIC in powder form *In vitro* drug release studies. Results of release studies are expressed as mean percentage ± standard error median of three independent experiments.

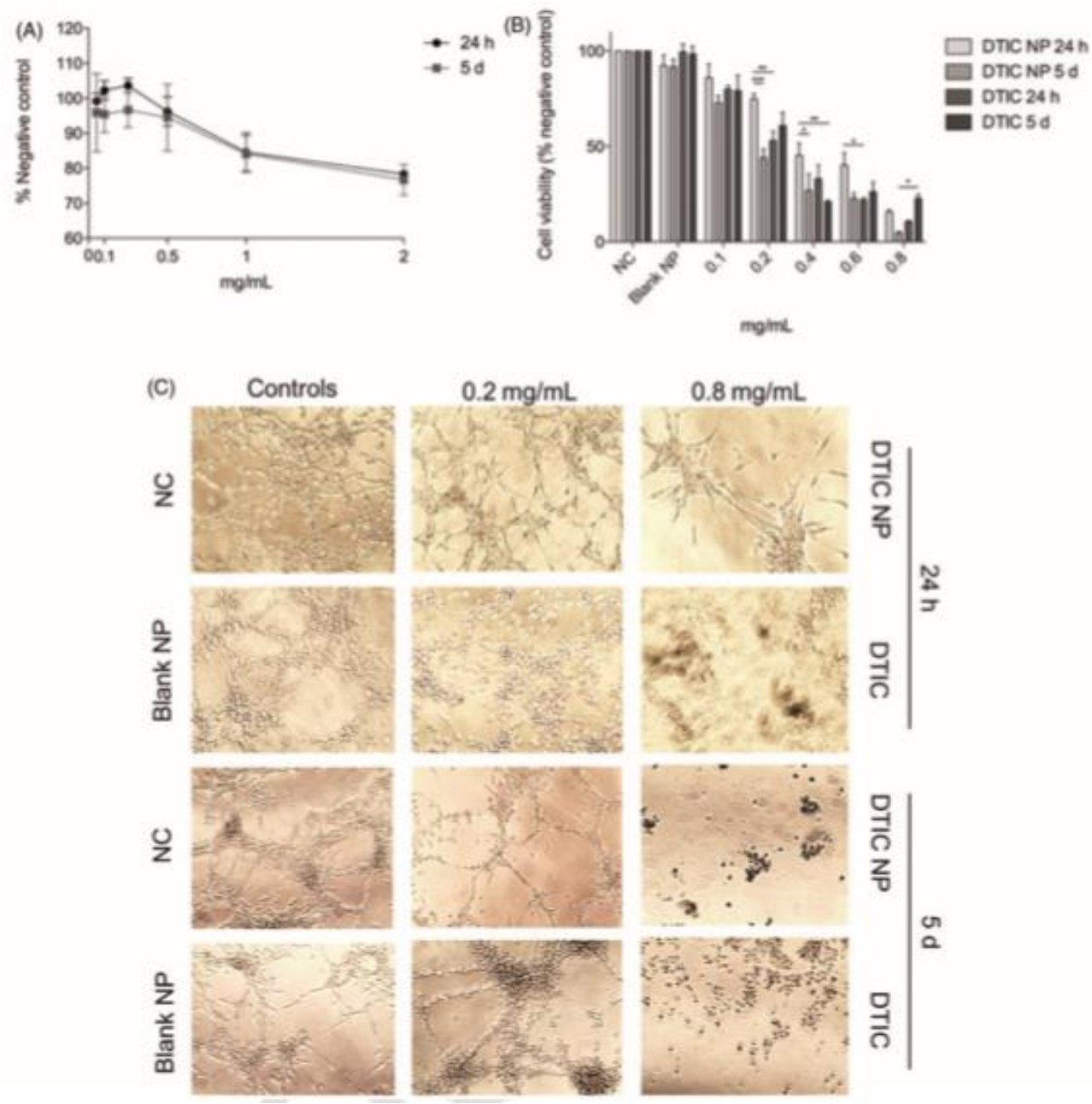

Figure 7: Cell Uptake evaluation **(A)** Cellular uptake of Rho-NP measured by spectrophotometry at 543 nm **(B, C)** Fluorescence intensity of Rho-NP and Rho solution. Results are shown as mean percentage in Rho-NP treated cells compared to Rho treated cells ± standard error median of three independent experiments.

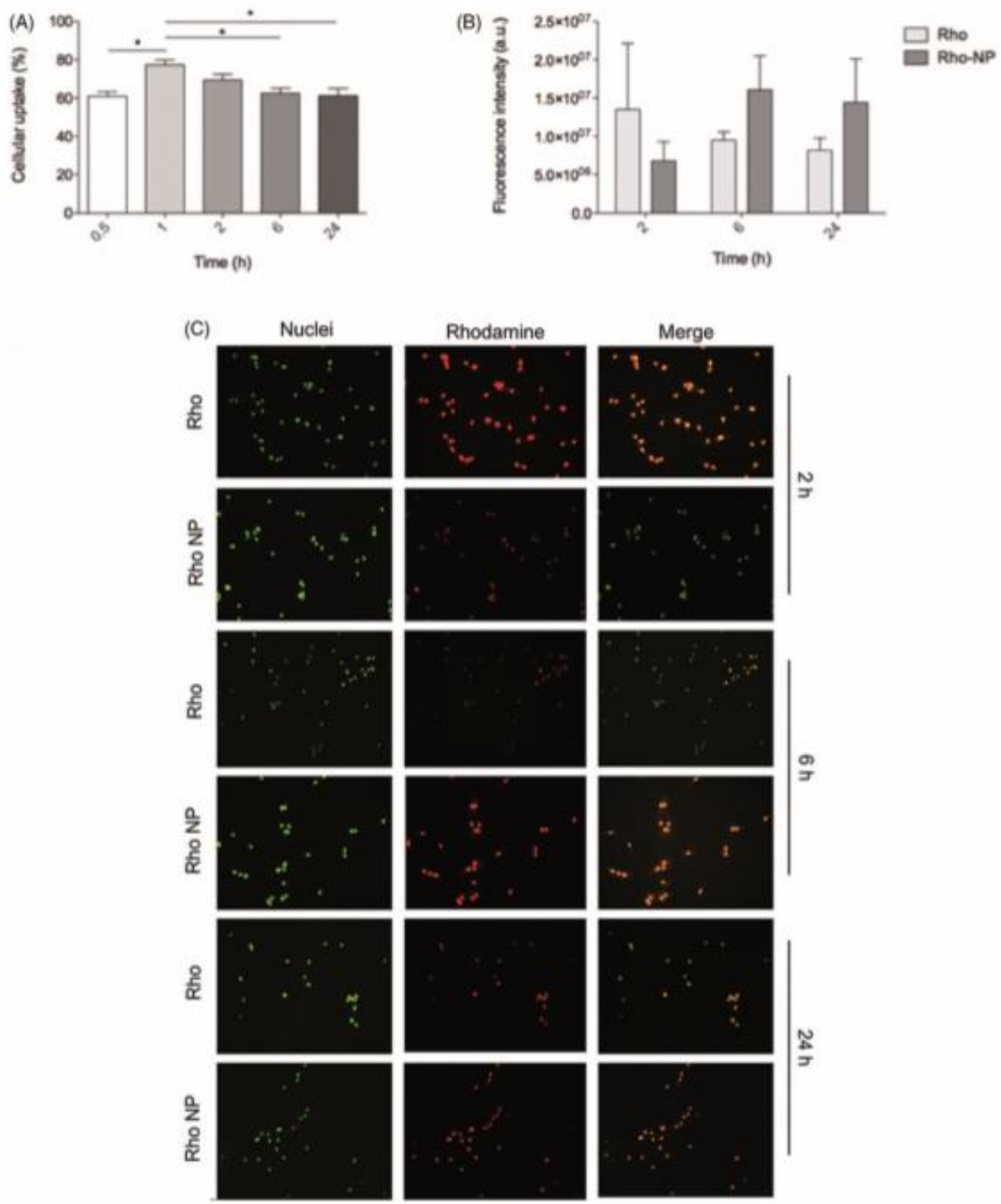

Figure 8: Cytotoxic effects of Blank NP, DTIC NP and DTIC in 3T3 and U87 cells after 24 h and 5 days exposure by MTT assay **(A)** Cytotoxic evaluation of Blank NPs in 3T3 cells **(B)** DTIC and DTIC NPs in U87 cells **(C)** U87 cells images over exposition to Blank NP, DTIC NP, DTIC and without treatment. The results are represented as mean percentage in blank NP, DTIC NP, DTIC treated cells compared to non-treated cells (negative control - NC) ± standard error median of three independent experiments.